Optimal Operating Point Manifolds in Active, Loaded Palladium Linked to Three Distinct Physical Regions

Mitchell Swartz
JET Energy, Inc. Wellesley, MA (USA)

Abstract - The three region hypothesis (3RH) resolves LANR systems into three different types, based on three different locations in solid state, loaded, metallic palladium or other Group VIII metal or alloy. 3RH is suggested by the multiplicity of OOP manifold groups and it is consistent with experimental data, palladium material science, and the multiple time constants previously reported which characterize 'heat after death'.

Index Terms - Optimal operating point, Three Region Hypothesis

1.1 Introduction - Lattice Assisted Nuclear Reactions are Real

Lattice assisted nuclear reactions [LANR] are real. Nuclear reactions can be assisted by an active metallic lattice which has been loaded with the isotopic fuel, creating an alloy such as PdD_x, if driven with adequate deuterium flux and a high enough loading ratio D/Pd [7,31,32]. LANR can produce more output heat than an ohmic control for the same electrical input, [called "excess heat"; 1,2,4,5,6,7], by reactions creating *de novo* nuclear products such as helium-4 [He^4, 3,8,10], tritium [9,11,15], and other isotopes [12,13,14]. $Pd/D_2O/Pt$ LANR devices, using OOP control (Figure 1) exhibit net energy gain, robust enough to drive functional Stirling engines. Corroboration has included heat flow measurement, redundant calorimetry [1,23], verified by thermal waveform reconstruction and noise measurement. Performance depends on loading rate, loading achieved, preparation of the sample, and its prehistory, including whether it was driven outside of the optimal operating point manifold, sample integrity, contamination, and materials which might quench performance [1]. IR imaging and thermometry (SPAWAR and JET Energy) indicate that the heat source is the cathode.

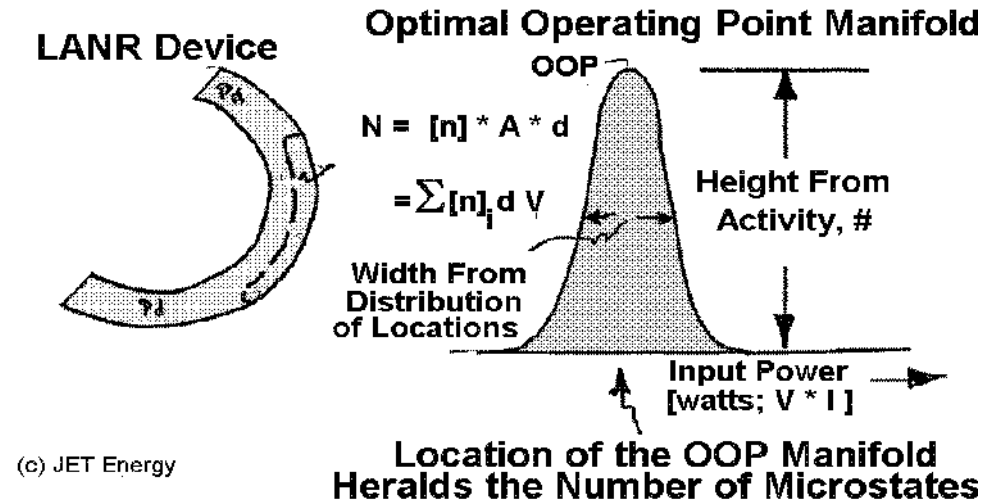

Figure 1. Correlation of LANR foci to an Optimal Operating Point manifold

3RH [24, 25] posits that successful, LANR [1,23] is generated in one of three (or more) different sites within the deuteron-loaded metal, including the palladium lattice (Figure 2). Each location has its own, differing, rate of excess heat, tritium, and helium production. Each location is linked to a different group of optimal operating point [OOP] manifolds which characterize active LANR samples and devices. The OOPs result from deuteron flux, best analyzed by the quasi-1-dimensional (Q1D) model of isotope loading.

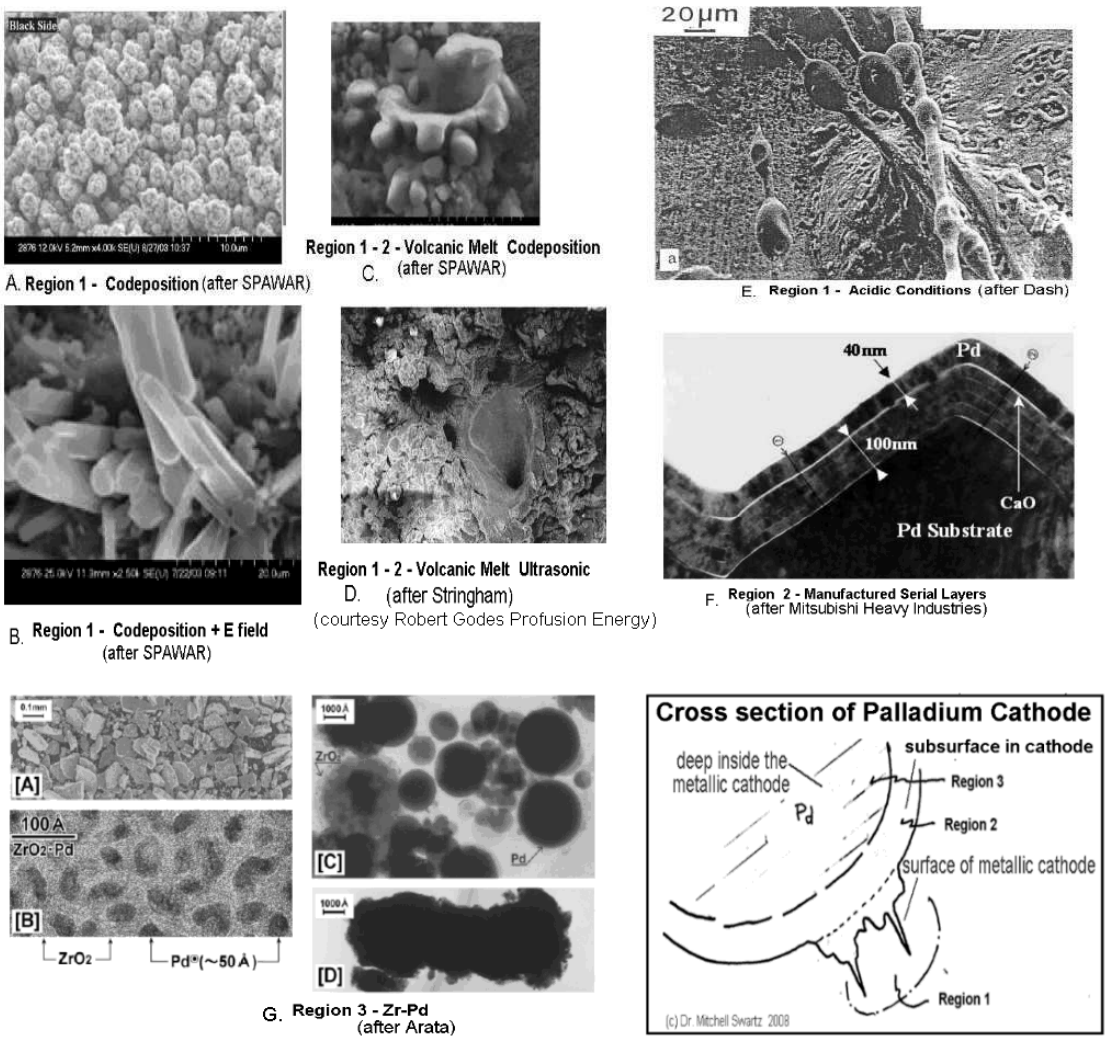

Figure 2. Three Types Palladium LANR sites (3RH Regions 1,2 and 3)

2.1 Background - Quasi-1-Dimensional Model of Deuteron Flux

Several of the difficulties of achieving LANR are explained by quasi-1-dimensional (Q1D) model of deuteron loading [17, 26-32]. Most importantly, the cold fusion/LANR deuteron-flux equation (Equation 1) teaches exactly why successful LANR is not simple electrolysis, as commonly taught. The deuteron fluxes include the bulk entry of deuterons (J_E) into the loading palladium, gas evolution (J_G) arising from the surface of the palladium, and the desired fusion reactions (J_F), if any. These three deuteron fluxes must be distinguished [26] at the surface of the low hydrogen-overvoltage Pd, with its surface populated with atomic, diatomic, and bulk-entering deuterons. Division of each deuteron flux by the local deuteron concentration yields the first-order deuteron flux constants, k_E, k_G, and k_F [with units of cm/sec, respectively].

$$k_e = \frac{B_D * qV}{L * [k_B * T]} - (\kappa_g + \kappa_f)$$

Equation 1

The first-order deuteron flux equation (Eq. 1) relates the three components of deuteron flux at the surface of a LANR device. The first order loading flux rate constant (k_E) is dependent on the applied electric field intensity minus the first order gas loss rate constant resulting from gas [D_2] evolution at the cathode (k_G). The first term of the Equation has geometric and material factors, L is the characteristic length, B_D is the diffusivity of the deuteron, and the ratio of two energies, the energy resulting from the applied electric field intensity (qV; where q is the electronic charge, and V is the applied voltage) and the energy resulting from thermal disorder (k_B*T; resulting from Boltzmann's constant k_B and temperature, T). Eq. 1 teaches what exactly controls loading, net bulk cathodic deuteron gain, and ultimately the desired LANR reactions. Equation 1 demonstrates that competitive gas-evolving reactions at the metal electrode surface destroy the desired reactions. It also shows how the ratio of the applied electric field energy to thermal energy [k_B*T] are decisive in controlling the loading flux of the palladium by deuterons. Successful LANR experiments are dominated by this ratio which reflects the 'war' between applied electrical energy which is organizing the deuterons versus their randomization by thermal disorganization.

2.2 Background - Q1D Result: LANR is Quenched by Electrolysis

NOTA BENE: The major implication of Equation 1 is that LANR reactions are quenched by electrolysis, which is opposite the conventional "wisdom" that LANR is 'fusion by electrolysis'. In fact, as Eq. 1 proves, the exact opposite is true [26]. The Q1D model's Deuteron Flux equation (Equation 1) reveals that the reason many of the critics and researchers missed LANR (other contamination or material issues) is that they were looking in the "wrong place". The equations predict that the ideal system involves a relatively low current, high electric field intensity, with small electrolysis (relative to loading and fusion) because the evolution of D_2 gas is mutually exclusive with the desired reactions [26].

2.3 Background - Optimal Operating Points (OOPs) and LANR

Optimal operating points and the OOP manifold groups appear when the calibrated output data of LANR (excess heat, excess power gain, or *de novo* incremental helium-4 or tritium production) is presented as a function of the input electrical power [1-10]. The optimal operating point (OOP) is the relatively narrow peak of the biphasic LANR production curve. The optimal operating point is but one focus at which the system can be driven. The rest of the foci, other possible points at which the system can be driven, are the "Optimal operating point manifolds". OOPs arise out of theoretical work from the quasi-one-dimensional (Q1D) model of isotope loading into a metal [26,27] which also gave rise to the codeposition [32].

Figure 3 shows an OOP manifold for a Pd Phusor®-type LANR device in heavy water accompanied by ohmic joule controls. The horizontal axis is the input electrical power, for 1 to 7 watts input. The vertical axis is the excess power output (watts). The peak output is near ~3.6

watts input power. Two regions of less than optimal output can be seen bordering the OOP, which occur because of inadequate loading (to the left of the peak) and wasteful electrolysis (to the right) [1,26,27].

2.4 Background - OOP Manifolds Are Important

OOPs and their manifolds are important for several reasons. First, LANR production data is much clearer as to origin and saliently better organized along the electrical input power axis (watts). Examined this way, it dispels the LANR "irreproducibility" myth, and what was disordered becomes ordered. Second, LANR is better controlled. Many early false "negative" LANR reports and widespread difficulties in observing the desired reactions are, in part, the result of failing to operate at the OOP [26,27,1,31,32]. Third, OOP understanding enables one to standardize examination of specimens and materials, normalizing treatment of samples. OOP characterization allows determination of maximal sample activity (MSA). Fourth, OOP manifolds appear to characterize most, if not all, of Pd-deuteride and other LANR systems (2), and explain a vast set of experimental data, not otherwise explicable. They have shown their worth by being proven useful to control LANR, photo-irradiation sensitivity of LANR cathodes [16,6], and "heat after death".

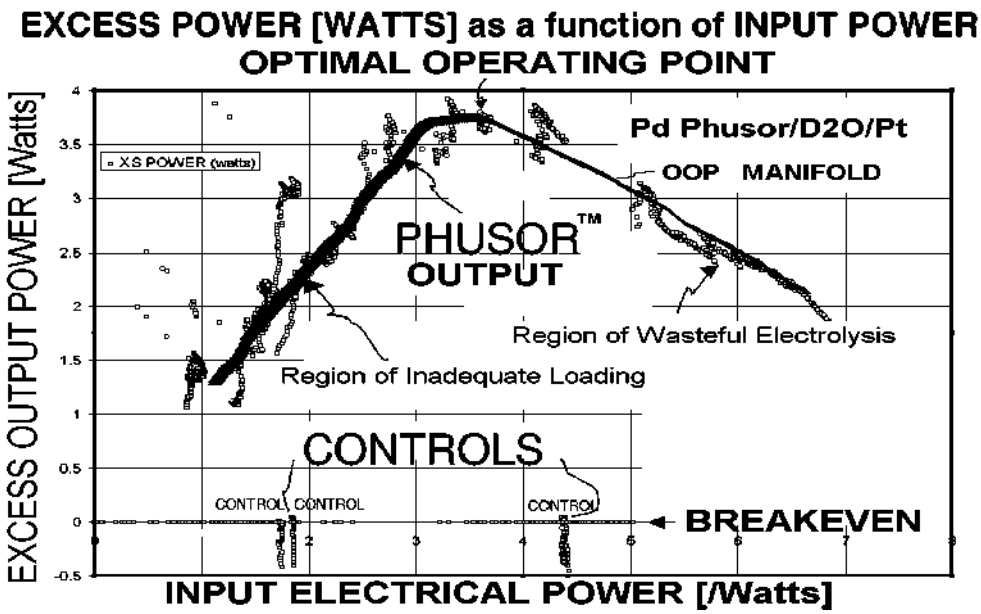

Figure 3. Optimal Operating Point (OOP) Manifold for Pd LANR Device

Thus, OOP manifolds, loading/loss ratios, and the qV/k_B*T ratio, in LANR systems are as fundamental as the understanding of frequency is to an electrical engineer or physicist. Once a student of science learns Fourier series - the transformation of time (seconds) to frequency (1/seconds or Hertz), there is no turning back. From this came, high fidelity audio systems, FM and spread-spectrum radio, etc. Similarly, in solid state physics and metallurgy, the transformation of distance (x) to "reciprocal space" (1/x) revealed a universe of Brillouin zones, Fermi energies, and activation energies from which there was no turning back. From this

has come transistors, computers, LEDs, etc. In this light, optimal operating points are such a transformation converting the time functions of applied voltage and electrical current to input electrical power.

2.5 Background - OOP Manifolds Are Universal

OOP manifolds describe a large group of LANR systems. OOPs and their manifolds appear to characterize most LANR systems [for products excess heat, tritium, and helium; 28-30]. OOPs characterize output for heavy water helium production, excess power gain from Pd/D_2O LANR systems and devices, for high impedance [$Pd/D_2O/Pt$, $Pd/D_2O/Au$] LANR devices, for excess heat in light water nickel systems, and $Ni/H_2OxD_2O_{1-x}/Pt$ and $Ni/H_2O_xD_2O_{1-x}/Au$] LANR devices, for codeposition systems and codeposition Phusor®-type LANR devices, for tritium generated from codeposition and "FPE" heavy water systems, and for commensurate excess heat and helium production in palladium-black systems [17, 28-30]. Figure 4 shows OOP manifolds from several independent investigators of excess power gain and incremental helium-4 and tritium production. The horizontal axis is the electrical power input [log watts]. The vertical axis is linear.

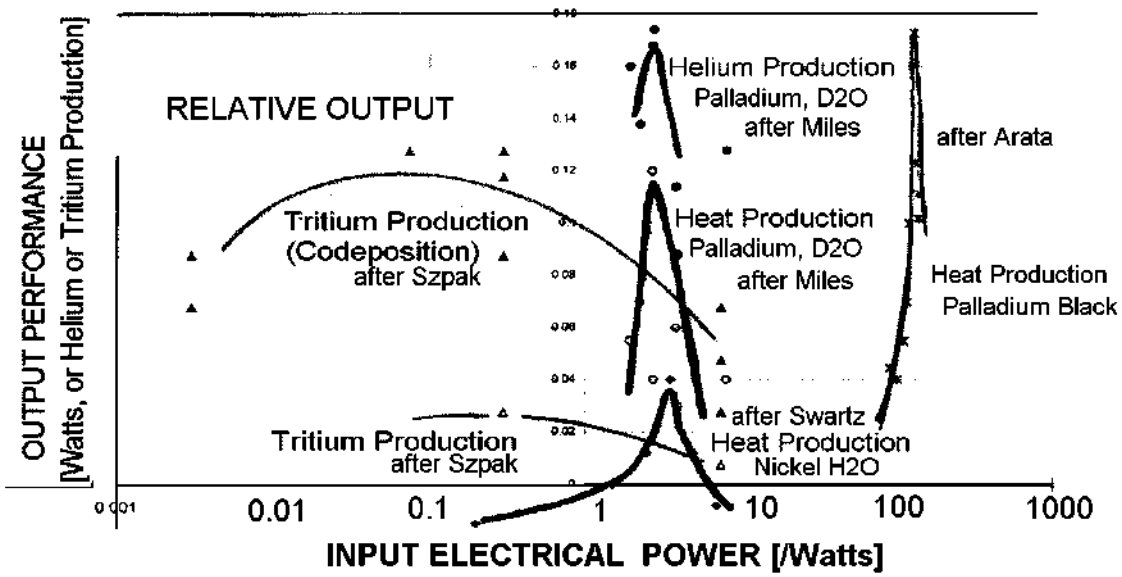

Figure 4. Multiple Optimal Operating Manifolds of Worldwide LANR Systems

3.1 3RH: Three Regions of LANR Behavior

Each palladium region looks different. At the top left of Figure 2 are shown palladium surface globules (A; produced by codeposition upon copper by Frank Gordon, Pamela Boss, and Larry Forsley [19]) involving at least several atomic layers. Palladium rods develop from the globules (B), produced after applied electric fields. This is region 1 in 3RH. To the top right of Figure 1 show morphologies (E) generated by acidic electrolysis generating nanotubes (courtesy of Prof. Dash [20]). This, too, is Region 1 in the 3RH hypothesis. The top middle image shows the occasional local melting of the palladium surface (C), presumably from the

desired reactions. Below it, in the center is a Pd melt cavity produced by cavitational LANR reactions (D) (after Roger Stringham [21]). The volcanic-like burst changes in Pd seen with SPAWAR codeposition and cavitation LANR in thin Pd foils loaded by "sonofusion" (Stringham) suggest melting and subsequent re-solidification of molten metal, reminiscent of nuclear fission fuel metal damage (spontaneous Californium "spike damage"). These show Region 1 and part of Region 2 in the 3RH hypothesis.

Below on the right bottom side are detailed Pd fabrication layers (F), 40 to 100 nanometers wide with a thin CaO layer intercalated (courtesy of Dr. Y. Iwamura [22]). These are Region 2 in the 3RH hypothesis.

Below on the left bottom side are Prof. Y. Arata's [3] nanomaterials (G) made from zirconium, leading to spherules superior to palladium black (courtesy of Talbot and Scott Chubb). These show Region 3 in the 3RH hypothesis.

3.2 3RH-OOP Interrelationship

The three different regions of LANR which are distinguished can be mapped onto Figure 4, as shown schematically in Figure 1. This shows three groups of OOP manifolds along the input electrical power axis. The 3RH connects each to a different site in the material.

REGION 1 - In Figure 4, the first group of OOP manifolds (Region 1) are on the left hand side. Region 1 involves the most superficial portions of the palladium, including surface dendrites and a variety of micro- and nano-particles, that characterize electrodeposited, and codeposited, palladium alloys involving at least several atomic layers. These surface sites, generated via codeposition and conventional LANR produce tritium.

REGION 2 - In Figure 4, the second group of OOP manifolds (Region 2) are in the central portion of the figure. Located deeper in the metal, subsurface Region 2 is metallic lattice physically located beneath Region 1, existing as a thin rim under the surface in the range of 40 microns to millimeters. Subsurface sites (Region 2) yield heat and helium production and transmutation products. They characterize conventional LANR ("FP") systems which make excess heat with commensurate helium production in palladium with heavy water, and excess heat with nickel systems in both light and heavy water.

REGION 3 - In Figure 4, the third group of OOP manifolds (Region 3) are on the far right side. Region 3 represents deeper sites in the deeper metallic lattice in the deep bulk or palladium-black systems which efficiently yield heat and helium production. Region 3 is less commonly involved in LANR, perhaps only in the very rare reports involving paroxysmal energy release from larger volumes. It appears to be involved with Arata's palladium black in dual cathodes [3].

This separation of LANR analysis into three sites might be quite important for two reasons. First, there may be disparate behavior for each site, with varying (possibly unique) products, rates, sensitivities, and problems. Second, such an analysis, allows semiquantitative measurements at each of the various locations involved.

3.3 3RH: Nature of 3RH-OOP Coupling

Figure 1 shows a schematic zone containing LANR foci (left) generating excess power, linked to one optimal operating point manifold (right). The relative height of the data points, which comprise each of the "Gaussian"-shaped OOP curves shown in Figures 3 and 4, is proportional to the product output, that is, the helium-4, tritium, or excess heat produced of a LANR specimen, material, or device driven at its OOP. The OOP height is thus a measure of the potential LANR activity of all available $N_{\#}$ microsites and their number. The applied electrical power couples to the LANR microsites, each of LANR activity, $A_{\#}$. That activity will be zero if the device or sample is not active, is nonfunctional, is driven improperly, is not loaded, or has fractured or deloaded, etc. Each active microsite receives a fraction $P_{\#}$/Pinput of the total input electrical power.

$$N_{\#} * P_{\#} = \text{Driving Power (watts)} = \text{Input Power Operating Point (IOP)} \qquad \text{[Eq. 2]}$$

3.4 Measurement of 3RH-OOP Coupling - The Excess Power Generation Equation

The modified, volume-corrected, multi-site, Excess Power Generation (EPG) equation connects the three groups of OOP manifolds to the three sites. We corrected and expanded Dave Nagel's surface monitoring equation [33] to the modified, volume-corrected, multi-site, Excess Power Generation (EPG) equation [24,25] for use with OOP manifolds [33,34] and for scientific use. The EPG shown in Equation 2 is a double summation (or double integral) where the summation is over each of the three regions, and over depth. The area is A. There is E energy per reaction and XSE is the excess energy, so dividing it by the time, T, yields the excess power, XSP.

$$XSE/T = \sum\sum\Big[[A * (\text{depth})] * Fvol * [N/(A* \text{depth-sec.})] * F_{theor} * E\Big] = XSP$$

Equation 3

Summation occurs over each of the sites, in the surface, subsurface and deep volume. The first term on the right hand side of the equation is the actual volume involved with active foci, followed by the fractional active palladium sites with defects etc., as required, within that volume, followed by the reactions per second at each of those sites within that volume, and finally a theoretical term (between zero and 1), and the energy per reaction (E, ~24 MeV per fusion reaction). F_{theor} represents several factors that control, or throttle, the coupling of the He^{4*} to the lattice. It varies from 0 to 1, and thus handles the coulomb barrier problem by using several theories and factors [35-42].

An actual LANR sample comprises a population of ~10^{20}-10^{22} candidate nuclei (among deuterons at ~1:1 ratio) which if active fuses ~10^{12} deuterons/second for each 1 watt of excess heat produced. The circa-21 to 24 MeV excited He^{4*} is coupled coherently with the loaded crystalline lattice by the optical phonons[42], consistent with Mossbauer effect [42-45]. The phonons, energies ~32-48 milli-eV in two bands [46-50], are the "oil" lubricating the transfer of energy from the excited nuclear state of helium to the lattice [1].

4.1 Theoretical Predictions of the 3RH Model

Prediction 1 - To test the 3RH hypothesis, expected output was generated, to be compared to what is observed (Figure 4). The volumetric ratio of the active sites was modeled as 5% of the total for the subsurface region (Region 2), and 1% of the total for the codepositional volume (Region 1). Figure 5 is the result of this first generated OOP from a model 3RH system in Pd. It can be seen that the 3RH-model generated OOP manifolds have a general qualitative agreement with what is actually observed for the locations of the OOP manifolds along the input electrical power axis (Figure 4). The match is non-quantitative, but suggestive. Furthermore, the 3RH OOP manifolds generated indicate that a wide variation in the distribution of foci density apparently exists in the codepositional region (Region 1). This may be possibly consistent with the great diversity of nanostructures of palladium (Figure 2). It can be seen that with further refinement a reasonable match to what is observed may be possible by the 3RH model.

Prediction 2 - Given the apparent success of generating something like the observed OOP manifolds from the 3RH model, a second prediction can be made. If the applied power is linked to the number of active sites, then as more active sites appear, for the same activity of the sites, the OOP manifold should swing to the right.

$$N_{\#} * A = XSP \text{ (excess power, watts)} \qquad \text{Equation 4}$$

This has been observed for LANR systems of both conventional, metamaterial Phusor®-type, and codepositional LANR systems as the excess heat increases during 'maturation' of the devices [1].

Prediction 3 - An additional prediction is that the height of each OOP manifold should increase as the manifold swings to the right, because with n-times more active sites (if the activity per site is maintained), then the height of the OOP manifold also increases by n-times. This has been observed, and reported [ICCF10].

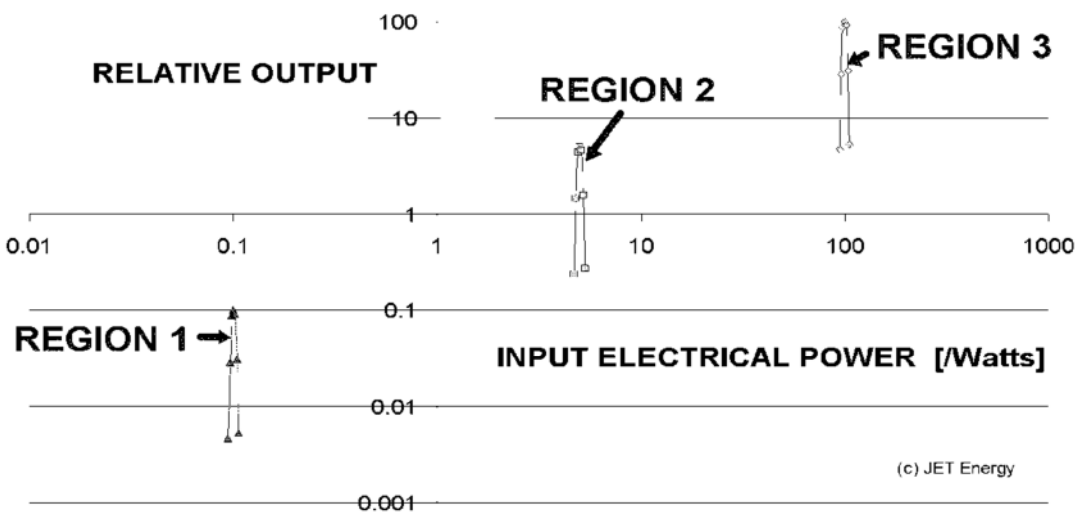

Figure 5 - Theoretically Derived Optimal operating point manifolds

4.2 Supportive Evidence - The 3RH is Consistent with Previous Reports

The 3RH is consistent with the known, unique material science, complex behavior of palladium [25], and its unusual binary alloy (hydrogen is a metal), a vast set of LANR experimental data [28-30], and with 'heat-after-death (HAD) excess heat' evanescent decay kinetics [2, 51,52]. These, and as the OOP manifolds corroborate (Figure 4) warrant consideration of the 3RH secondary to a variety of LANR sites. Palladium is a unique metal [53-57] discussed in considerable detail elsewhere [25] and has a behavior pattern consistent with the 3RH hypothesis. The time derivative of the excess energy "heat after death" [HAD, 57,2] is the tardive thermal power (TTP). TTP produces HAD, which is a heterodyne "excess" energy which continues to be generated even AFTER the input electrical energy is shut off. The poorly-chosen term 'Death' referred to the termination of input electrical power in Pons' cell, which by definition occurs in the HAD region. In the original "HAD" reported by Pons and Fleischman, the electrolysis cell had finally run out of heavy water (due to the electrolysis) thereby unintentionally and inadvertently creating the region of no further input electrical power, because the electrical circuit was 'open circuited'.

We previously reported at ICCF10, and thereafter, that TTP information was resolvable using high impedance Phusor®-type LANR devices and "Dual ohmic control calorimeters" after they were loaded, activated, and driven at their OOP [28-30], and analyzed for their kinetics [51,52]. Tardive thermal power (TTP) appeared to occur in palladium in heavy water, but much less so in nickel with "pure" light water for JET Energy Phusor®-type spiral wound cold fusion cathodes. Furthermore, we have used lumped parameter electrical analysis of the TTP-active system. The loaded active palladium lattice's deuteron-loading capacitance is ~64 micromoles per volt*. The systems' admittance for the desired excess enthalpy TTP reactions is ~7 picomoles/[sec-volt*], and that capacitance is dwarfed by the system's deloading admittance for loss of deuterons by outgas which is ~15 nanomoles/[sec-volt*]. The kinetics reveals HAD evanescent heat generated by two (or more) sites [24,51,52]. Most of the sites have TTP which falls off with a time constant of several minutes, but some of the sites had a time constant of ~20 minutes to hours [51,52]. This is consistent with vicinal surface [16] and deeper [1,2] sites, with the longer time constant secondary to the deeper location within the lattice. We suggested in 2005, a two-site TTP reaction system in the palladium heavy water Phusor system. This was felt to be consistent with both deep, and the more superficial, perhaps ~100 micrometers from the surface, sites previously suggested both in our data and in other codepositional results [1,16].

5. CONCLUSION

With the three region hypothesis (3RH), there is an attempt to resolve the observed output of LANR systems and devices into three different types, at three different physical locations, or sites, in the solid state, loaded, active, metallic palladium lattice. 3RH links each of these physical locations to one of three specific groups of OOP manifolds, which appear when analyzing LANR output as function of input electrical power.

3RH is suggested by existence of three OOP manifold groups, which appear to characterize all known LANR samples and systems [28-30]. 3RH is consistent with experimental data,

including the material science and complex behavior of palladium [25], and our previous reports of (at least) two time constants characterizing 'heat after death' excess heat [2, 51, 52].

3RH enables potentially active LANR regions on a physical specimen to be better analyzed, with deconvolution of each site's differing excess heat, tritium, and helium production rates. 3RH may better enable LANR to be examined semiquantitatively by the Excess-Power-Generation (EPG) equation [24, 33, 34]. 3RH analysis with the EPG equation appears to be helpful in the analysis of LANR excess heats [1,2] correlated with near-IR detection emission in 2-D.

Acknowledgments

The author thanks Gayle Verner for her meticulous help in manuscript and idea development, and also Drs. Yasuhiro Iwamura, Frank Gordon, Pam Boss, Larry Forsley, Stan Szpak, Roger Stringham, Talbot Chubb, Robert Godes, Scott Chubb, Peter Hagelstein, David Nagel, Jeff Tolleson and Richard Kramer for their helpful conversations, and JET Energy and New Energy Foundation for their additional support. PHUSOR® is a registered trademark of JET Energy, Incorporated. Hyperdrive™ and PHUSOR®-technology are protected by U.S. Patents D596724, D413659 and U.S. Patents pending. All rights reserved. © 2010 JET Energy, Incorporated

REFERENCES

1. M. Swartz, G. Verner, "Excess Heat from Low Electrical Conductivity Heavy Water Spiral-Wound Pd/D2O/Pt and Pd/D2O-PdCl2/Pt Devices", Condensed Matter Nuclear Science, Proceedings of ICCF-10, eds. Peter L. Hagelstein, Scott, R. Chubb, World Scientific Publishing, NJ, ISBN 981-256-564-6, 29-44 (2006).
2. M. Swartz, G. Verner, "Dual Ohmic Controls Improve Understanding of 'Heat after Death'", Transactions American Nuclear Society, vol. 93, ISSN:0003-018X, 891-892 (2005).
3. Y. Arata and Y.C. Zhang, 'Anomalous Production of Gaseous 4He at the Inside of DS-Cathode During D2-Electrolysis', Proc. Jpn. Acad. Ser. B, Vol. 75, p. 281 (1999); Arata, Y. and Y.C. Zhang, Observation of Anomalous Heat Release and Helium-4 Production from Highly Deuterated Fine Particles. Jpn. J. Appl. Phys. Part 2, 1999. 38: p. L774; Arata, Y. and Y. Zhang, The Establishment of Solid Nuclear Fusion Reactor. J. High Temp. Soc., 2008. 34(2): p. 85.
4. I. Dardik, H. Branover, A. El-Boher, D. Gazit, E. Golbreich, E. Greenspan, A. Kapusta, B. Khachatorov, V. Krakov, S. Lesin, B. Michailovitch, G. Shani, and T. Zilov, 'Intensification of Low Energy Nuclear Reactions Using Superwave Excitation', Proceedings of the 10th International Conference on Cold Fusion (2003).
5. M. Fleischmann, S. Pons, "Electrochemically Induced Nuclear Fusion of Deuterium", J. Electroanal. Chem., 261, 301-308, erratum, 263, 187 (1989); M. Fleischmann, S. Pons, "Some comments on the paper Analysis of Experiments on Calorimetry of LiOD/D2O Electrochemical Cells, R.H.Wilson et al., J. Electroanal. Chem., 332 (1992) 1* ", J. Electroanal. Chem., 332, 33-53, (1992); M. Fleischmann, S. Pons, "Calorimetry of the Pd-D2O system: from simplicity via complications to simplicity", Physics Letters A, 176, 118-129, (1993); M. Fleischmann, S. Pons, M. Anderson, L.J. Li, M. Hawkins, "Calorimetry of the palladium-deuterium-heavy water System", Electroanal. Chem., 287, 293, (1990).

6. D. Letts and D. Cravens, “Laser Stimulation of Deuterated Palladium: Past and Present”, Proceedings of the 10th International Conference on Cold Fusion (2003).
7. M. McKubre, F. Tanzella, P. Hagelstein, K. Mullican, and M. Trevithick, ‘The Need for Triggering in Cold Fusion Reactions,’ Proc. 10th International Conf. on Cold Fusion (2003).
8. M.H., Miles, R.A. Hollins, B.F.Bush, J.J. Lagowski, R.E. Miles, “Correlation of excess power and helium production during D2O and H2O electrolysis”, J. Electroanal. Chem., 346 (1993) 99-117; Miles, M.H., B.F.Bush, “Heat and Helium Measurements in Deuterated Palladium”, Transactions of Fusion Technology, vol 26, Dec. 1994, pp 156-159.
9. M. Srinivasan, et alia., “Tritium and Excess Heat Generation During Electrolysis of Aqueous Solutions of Alkali Salts with Nickel Cathode,” Frontiers of Cold Fusion, Ed. by H. Ikegami, Proceedings of the Third International Conference on Cold Fusion, October 21-25, 1992, Universal Academy Press, Tokyo, pp 123-138.
10. V. Violante, E. Castagna, C. Sibilia, S. Paoloni, and F. Sarto, ‘Analysis of Mi-Hydride Thin Film After Surface Plasmons Generation by Laser Technique’ ‘ Proceedings of the 10th International Conference on Cold Fusion (2003).
11. F. G. Will, K. Cedzynska, D.C. Linton, “Tritium Generation in Palladium Cathodes with High Deuterium Loading”, Transactions of Fusion Technology, vol 26, Dec. 1994, pp 209-213; “Reproducible tritium generation in electrochemical cells employing palladium cathodes with high deuterium loading, J. Electroanal. Chem 360 (1993) 161-176.
12. S. Szpak, P.A. Mosier-Boss, C. Young, and F.E. Gordon, ‘Evidence of Nuclear Reactions in the Pd Lattice’, Naturwissenschaften, Vol. 92, pp. 394-397 (2005).
13. S. Szpak, P.A. Mosier-Boss, and F.E. Gordon, ‘Further Evidence of Nuclear Reactions in the Pd/D Lattice, Naturwissenschaften, Vol. 94, pp. 511-514 (2007).
14. P.A. Mosier-Boss, S. Szpak, F.E. Gordon, and L.P.G. Forsley, ‘Use of CR-39 in Pd/D Co-Deposition Experiments’, European Physics Journal-Applied Physics, Vol. 40, pp. 293-303 (2007).
15. S. Szpak, P.A. Mosier-Boss, R.D. Boss, and J.J. Smith, ‘On the Behavior of the Pd/D System: Evidence for Tritium Production’, Fusion Technology, Vol. 33, pp. 38-51 (1998).
16. M. Swartz, G. Verner, “Photoinduced Excess Heat from Laser-Irradiated Electrically-Polarized Palladium Cathodes in D2O”, Condensed Matter Nuclear Science, Proc. ICCF-10, eds. Peter L. Hagelstein, Scott Chubb, NJ, ISBN 981-256-564-6, 213-226 (2006).
17. M. Swartz, “Consistency of the Biphasic Nature of Excess Enthalpy in Solid State Anomalous Phenomena with the Quasi-1-Dimensional Model of Isotope Loading into a Material”, Fusion Technology, 31, 63-74 (1997).
18. Szpak, S., P.A. Mosier-Boss, and F. Gordon, Further evidence of nuclear reactions in the Pd lattice: emission of charged particles. Naturwiss., DOI 10.1007, (2007).
19. Szpak, S., et al., The effect of an external electric field on surface morphology of co-deposited Pd/D films. J. Electroanal. Chem., 580: 284-290, (2005).
20. Dash, J. and D.S. Silver. Surface Studies After Loading Metals With Hydrogen And/Or Deuterium, 13th Conf. CMNS 2007. Sochi, Russia; Dash, J. and S. Miguet, Microanalysis of Pd Cathodes after Electrolysis in Aqueous Acids. J. New Energy, 1996. 1(1): p. 23.
21. Stringham, R., Cavitation and Fusion, ICCF-10. 2003. Cambridge, MA
22. Iwamura, Y., M. Sakano, and T. Itoh, Elemental Analysis of Pd Complexes: Effects of D2 Gas Permeation. Jpn. J. Appl. Phys. A, 2002. 41: p. 4642; Iwamura, Y., et al., “Observation Of Surface Distribution Of Products By X-Ray Fluorescence Spectrometry During D2 Gas

Permeation Through Pd Complexes", in The 12th International Conference on Condensed Matter Nuclear Science. 2005. Yokohama, Japan.
23. Swartz, M.R. "Excess Power Gain and Tardive Thermal Power Generation using High Impedance and Codepositional Phusor Type LANR Devices", Proceedings of the 14th International Conference on Condensed Matter Nuclear Science (2010)
24. M. Swartz, "Spatial and Temporal Resolution of Three Sites Characterizing Lattice-Assisted Nuclear Reactions", APS 2008; Swartz, M., "Colloquium on LANR in Deuterated Metals Colloquium on LANR at MIT, August 2007.
25. Three Physical Regions of Anomalous Activity in Deuterided Palladium Mitchell Swartz, Infinite Energy, Vol. 14, Issue 61, 19-31 (2008).
26. M. Swartz, "Quasi-One-Dimensional Model of Electrochemical Loading of Isotopic Fuel into a Metal", Fusion Technology, 22, 2, 296-300 (1992).
27. M. Swartz, "Isotopic Fuel Loading Coupled to Reactions At an Electrode", Fusion Technology, 26, 4T, 74-77 (1994).
28. M. Swartz, "Generality of Optimal Operating Point Behavior in Low Energy Nuclear Systems", Journal of New Energy, 4, 2, 218-228 (1999).
29. M. Swartz, "Optimal Operating Point Characteristics of Nickel Light Water Experiments", Proceedings of ICCF-7 (1998).
30. M. Swartz, "Control of Low Energy Nuclear Systems through Loading and Optimal Operating Points", ANS/ 2000 Int. Winter Meeting, Nov. 12-17, 2000, Washington, D.C. (2000).
31. M. Swartz, "Patterns of Failure in Cold Fusion Experiments", Proceedings of the 33RD Intersociety Engineering Conference on Energy Conversion, IECEC-98-I229, CO, Aug. (1998).
32. M. Swartz, "Codeposition Of Palladium And Deuterium", Fusion Technology, 32, 126-130 (1997).
33. D. Nagel, ICCF13, Sochi, Russia, ""Powers, Materials and Radiations from Low Energy Nuclear Reactions on Surfaces" (2007).
34. Swartz, M.R., Gayle Verner, Alan Weinberg, "Possible Non-Thermal Near-IR Emission Linked with Excess Power Gain in High Impedance and Codeposition Phusor-LANR Devices", in Fourteenth International Conference on Cold Fusion. 2008. Washington, DC.
35. Rabinowitz, M., et al. Opposition and Support for Cold Fusion. in Fourth International Conference on Cold Fusion, Lahaina, Maui: Electric Power Research Institute 3412 Hillview Ave., Palo Alto, CA 94304, (1993).
36. M. Swartz, "Possible Deuterium Production From Light Water Excess Enthalpy Experiments using Nickel Cathodes", Journal of New Energy, 3, 68-80 (1996).
37. Widom, A., Larsen, L, "Ultra Low Momentum Neutron Catalyzed Nuclear Reactions on Metallic Hydride Surfaces," Eur. Phys. J. C, (2006).
38. Hagelstein, P.L., Coherent and semicoherent neutron transfer reactions III, Fusion Technol., 23, 353, (1993).
39. Chubb, S.R. and T.A. Chubb, The Role of Hydrogen Ion Band States in Cold Fusion. Trans. Fusion Technol., 26(4T), 414.(1994).
40. T.A. Chubb, S.R.Chubb, "Ion Band States: What they are, and How they Affect Cold Fusion", Cold Fusion Source Book, ibid., 75, (1994).
41. Chubb, S.R. and T.A. Chubb. An Explanation of Cold Fusion and Cold Fusion By-products, based on Lattice Induced Nuclear Chemistry. in Second Annual Conference on Cold Fusion, "The Science of Cold Fusion". Como, Italy: Societa Italiana di Fisica, Bologna, Italy, (1991).

42. M. Swartz, “Phusons in Nuclear Reactions in Solids”, Fusion Technology, 31, 228-236 (1997).
43. Gibb, T.C., “Principles of Mossbauer Spectroscopy”, Chapman and Hall, London (1974).
44. Dickson, D.P.E., Berry, F., “Mossbauer Spectroscopy”, Cambridge University Press (1983).
45. U. Gonser, “Mossbauer Spectroscopy”, Springer-Verlag, NY (1975).
46. D. A. Papaconstantopoulos, B.M. Klein, et alia, “Band structure and superconductivity of PdDx and PdHx”, Physical Review, 17, 1, 141150, (1977).
47. E. Wicke, H. Brodowsky, “Hydrogen in Palladium and Palladium Alloys”, Hydrogen in Metals II, G. Alefield, J. Volkl, Eds., Springer, Berlin (1978).
48. H. Teichler, “Theory of hydrogen hopping dynamics including hydrogen-lattice correlations”, J. Less-Common Metals, 172-174 (1991) 548-556.
49. B. M. Klein, R. E. Cohen, “Anharmonicity and the inverse isotope effect in the palladium-hydrogen system”, Phys. Rev. B, 45, 21, 405 (1992).
50. R.W. Bussard, “Virtual-State Internal Nuclear fusion in Metal Lattices”, Fusion Technology, 16, 231-236 (1989).
51. M. Swartz, G. Verner, “Two Site of Cold Fusion Reactions Viewed by their Evanescent Tardive Thermal Power”, Abstract ICCF-11 (2004); M. Swartz, “Kinetics and Lumped Parameter Model of Excess Tardive Thermal Power”, Mitchell Swartz, APS (2005).
52. M. Swartz, “Kinetics and Lumped Parameter Model of Excess Tardive Thermal Power”, Mitchell Swartz, APS (2005).
53. http://www.stillwaterpalladium.com/history.html http://diamonds-jewelry-gems.blogspot.com/2008/04/understanding-palladium-and-being-able.html http://www.jstor.org/pss/208418
54. Hampel, C.A., “Rare Metal Handbook”, Reinhold Pub., NY (1954).
55. S. Pons, Fleischman, M., “Heat After Death,” Proc. ICCF-4, Maui, EPRI TR104188-V2, vol. 2, 8-1 (1994); Trans. Fusion Technology, 26, Number 4T, Part 2, p. 87 (December 1994).
56. Case, L.C. Catalytic Fusion of Deuterium into Helium-4. in The Seventh International Conference on Cold Fusion., Vancouver, Canada: ENECO, Inc., Salt Lake City, UT. (1998).
57. Cotton, F.A, G.Wilkinson, “Advanced Inorganic Chemistry”, Interscience, NY (1972).